Precursors to flutter instability by an intermittency route: a model free approach

J. Venkatramani[a], Vineeth Nair[b], R.I. Sujith[b], Sayan Gupta[a], Sunetra Sarkar[b,*]

[a] *Department of Applied Mechanics, Indian Institute of Technology Madras, Chennai 600036 India*
[b] *Department of Aerospace Engineering, Indian Institute of Technology Madras, Chennai 600036 India*

Abstract

The aeroelastic response of a NACA 0012 airfoil in the flow regimes prior to flutter is investigated in a wind tunnel. We observe intermittent bursts of periodic oscillations in the pitch and plunge response, that appear in an irregular manner from a background of relatively lower amplitude aperiodic fluctuations. As the flow speed is increased, the intermittent bursts last longer in time until eventually transitioning to a fully developed periodic response, indicating the onset of flutter. The repeating patterns in the measured response are visualized using recurrence plots. We show that statistics of the recurrence states extracted from these plots can be used to develop model-free precursors that forewarn an impending transition to flutter, well before its onset.

Keywords: Wind tunnel experiments, Intermittency, Recurrence, Aeroelastic flutter, Precursor to flutter

*Corresponding author:sunetra.sarkar@gmail.com, Phone: +91 44 2257 4024, FAX: +91 44 2257 4024

1. Introduction

Aeroelastic flutter is an instability that occurs when the aerodynamic forces overcome the structural and inertial forces in slender flexible structures, such as aircraft wings, giving rise to large amplitude periodic oscillations. Classical flutter — also known as coupled-mode or bending-torsion flutter — involves a fluid-elastic coupling between the structural modes, wherein above a critical wind speed, energy is transferred from the flow to the structure (Fung, 1955). This energy transfer leads to self-sustaining limit cycle oscillations (LCO) that can cause either an abrupt structural failure due to overloading, or fatigue failure due to gradual accumulation of damage. It is therefore obvious that the onset of flutter poses a risk to the structure integrity, and consequently an important criterion in design and maintenance is that the operating conditions should not lead to flutter instability. Aeroelastic instabilities are not restricted to aircraft wings alone. The blades of modern wind turbines are also susceptible to aeroelastic flutter (Lobitz, 2004; Zhang and Huang, 2011). Understanding, predicting and preventing the onset of flutter has therefore remained a focal point of extensive research, especially in the past decades.

Stability characteristics and bifurcation behaviour of aeroelastic systems having both structural and aerodynamic nonlinearities have been extensively investigated in the literature (Alighanbari and Price, 1996; Lee et al., 1999; Dowell and Tang, 2002; Sarkar and Bijl, 2008). Significant research effort has also been invested in identifying and modeling various types of nonlinearities (Abdelkefi et al., 2012). These studies were primarily aimed towards developing an understanding of the expected nonlinear aeroelastic response

and its underlying physics. However, the high costs associated with structural failures and the expenditures incurred towards preventive maintenance, scheduling and retrofitting, there is a need to develop methodologies for identifying the onset of flutter.

Early studies devoted to the development of methodologies for identifying the flutter boundary focussed on estimating the damping in the fluid-structure interaction system (Kehoe, 1985; Cox et al., 2006). However, damping based approaches are unsuitable for structures with complex, nonlinear damping. The other traditional approach for flutter prediction is based on the estimation of dynamical stability. Zimmerman and Weissenburger (1964) proposed a methodology to derive a flutter margin based on the Routh's stability criterion (Fung, 1955), which was applied to a two degree of freedom system under the assumption of quasi-steady aerodynamics. Later, the Zimmerman - Weissenburger Methodology (ZWM) was also applied in systems with higher degrees of freedom (Price and Lee, 1993). Recently, an extension of ZWM was presented by Poirel et al. (2005), using uncertainty quantification for a more reliable estimate of the modal parameters. Flutter margin prediction approach based on Jury's stability criterion for digitalized systems has been documented by Matsuzaki (2011). An on-line flutter prediction tool called flutterometer was developed by Lind and Brenner (2000) using an analytical model. To account for modeling errors and uncertainties, parts of the model were updated through a nonlinear iterative algorithm that generates a "worst case flutter boundary". Although this technique is robust, the stability margins tend to be quite conservative (Strganac and Platanitis, 2001).

The literature review reveals that the existing methodologies for predicting the flutter boundaries require the development of a mathematical model. Moreover, an accurate and early on-line prediction of the onset of flutter using measurements directly remain elusive. This study aims towards developing a methodology for identifying the flutter boundary directly from measurement data of the response of the system. The development of these precursors follows from time series analysis of the response measurements, where the onset of LCOs are presaged by a transitional intermittent state.

Studies on identifying precursors to undesirable states in other nonlinear systems are available in the literature. Precursors to instabilities have been obtained by forcing the dynamical system with broad band noise (Wiesenfeld, 1985; Surovyatkina, 2005). The noise gets selectively amplified at the instability frequency and the width of the dominant frequency is considered as an indicator of instability (Wiesenfeld, 1985). Further, Surovyatkina (2005) has shown for a nonlinear geophysical system that the width of the hysteresis zone gets reduced as the noise levels are increased. Both these studies were developed in the frequency domain. However, a frequency domain analysis might not always be sufficient to identify precursors as external stochastic forcing can change the dynamics qualitatively, as was shown for a thermoacoustic system by Jegadeesan and Sujith (2013).

The focus of the present study is to identify robust precursors to flutter instability through an intermittent state of response in an essentially model-free approach. This is done by studying the characteristics of the aeroelastic response at conditions prior to the onset of flutter. Experimental measures are obtained from wind tunnel tests. The responses are measured

at regimes of both stable (no flutter) and unstable (flutter) operations by systematically increasing the mean flow velocity. The transition to instability happens through an intermittent regime which has a specific dynamical signature, based on which precursors to impending flutter are developed. As the precursors are developed based on the measured response, the technique is essentially model independent, the advantages of which are elaborated later in the paper.

The organization of the paper is as follows: A brief overview of intermittency and its appearance in other models and engineering systems is presented in Section 2. Section 3 describes the experimental setup and provides a primer on the computational techniques presented in the paper. Precursors to flutter are developed from the measured pitch and plunge response using recurrence quantification analysis in Section 4. The proposed developments are subsequently illustrated in Section 5 through a numerical example and provides a validation of the developed precursors in predicting the onset of flutter. The salient features of this study are summarized in Section 6.

Nomenclature

b	semi-chord of airfoil
c	chord length
d	embedding dimension
d_0	optimum embedding dimension
$E_1(d), E(d)$	measures used to compute d_0
$E_2(d)$	measure used to check for determinism in signals
f_s	under sampled frequency (Hz)

f_v	dominant frequency (Hz)
I_α	pitch moment of inertia kgm^2
k_y	stiffness in plunge (N/m)
k_α	stiffness in pitch (Nm/rad)
m_1	mass of the plunging frame (Kg)
m_2	mass of the pitching mechanism (Kg)
m_3	mass of the airfoil (Kg)
m_y	total mass in plunge ($m_1 + m_2 + m_3$) (Kg)
m_α	total mass in rotation ($m_2 + m_3$) (Kg)
S	static unbalance (Kg-m)
N	length of time series
U	wind flow speed (m/s)
y	plunge response (mm)
α	pitch response (deg)
ϵ	threshold for constructing recurrence plot
ζ_y	viscous damping ratio in plunge
ζ_α	viscous damping ratio in pitch
ω_y	natural frequency in plunge (Hz)
ω_α	natural frequency in pitch (Hz)
ϖ	ratio of plunge to pitch natural frequencies
r	radius of gyration
μ	nondimensional mass
V	nondimensional wind speed ($U/b\omega_\alpha$)
x_α	nondimensional distance between elastic axis and centre of mass

a_h	nondimensional distance from the mid-chord to the elastic axis
τ	time delay for embedding
τ_{opt}	optimum time delay for embedding

2. Intermittency

Intermittency refers to the occurrence of a signal that irregularly alternates between regular phases and irregular bursts (Schuster and Just, 2006). In general, for a dynamical system, intermittency can be thought of as analogous to a fluctuation between two stable states for certain ranges of control parameter in the system. For example, the two stable states could be a fixed point and a stable limit cycle. Pomeau and Manneville (1980) presents three types of intermittency, termed as type I-III to describe the route to chaos from a periodic state. Each type of intermittency corresponds to a bifurcation taking place in the system. Intermittency has been observed in several physical systems and have been widely reported in the literature (Richardson, 1993; Ott and Sommerer, 1994; Covas et al., 2001; Grebogi et al., 1987; Price and Mullin, 1991; Bauer et al., 1992; Kabiraj and Sujith, 2012; Nair et al., 2014).

From an aeroelastic perspective, one of the earliest observations on intermittent responses in nonlinear aeroelastic systems was reported by Price and Keleris (1996). Numerical simulations were performed to study the dynamic stall in a NACA 0012 airfoil and the presence of aerodynamic nonlinearity through a complex stall model showed chaotic behaviour. Two types of re-

sponses were discussed, one of them was reported as "intermittent chaos" in which short intermittent chaotic bursts after long periodic regimes were observed. The system also returned to different periodic attractors after the short chaotic spells. The source of this intermittency behaviour was not known, nor their routes for the stall flutter model were analyzed. In a later numerical study, Poirel (2001) examined the dynamics of a structurally nonlinear pitch plunge aeroelastic model in the presence of wind turbulence. The system dynamics were discussed in terms of the response probability density functions (pdf) and the qualitative changes in them. The pdf were observed to transition from stochastic damped to stochastic LCO type response. However, the author noticed difficulties in categorizing the response time histories into these precise groups as the time histories showed bursts in both and there were no sharp distinctions. At mean wind speeds much below the stochastic LCO behaviour, bursts of periodic regimes were observed in the time domain. The duration of the bursts were observed to increase with an increase in the mean wind velocity. The author referred to this strange time domain behaviour as "on-off" intermittency (Yoon and Ibrahim, 1995). However, these intermittent time histories did not show up as a qualitative change in the response pdf and no further investigations were carried out. Similar observations were made experimentally when blunt objects were placed ahead of a wing in a wind tunnel experiment (Poirel et al., 2008). Intermittency was also reported in experiments on few other aeroelastic systems, e.g., in a bridge deck flutter (Andrianne and Dimitriadis, 2011) and in a delta wing (Korbahti et al., 2011). However, intermittency is still largely an unexplored area in aeroelasticity and none of these studies have

attempted to analyze its dynamics in detail.

Further, within the aeroelastic community, none of the previous works have investigated the ability of intermittency to forewarn an impending instability. Recently, for a turbulent combustor, Nair et al. (2014) has demonstrated that recurrence plots obtained from a short time signal can be successfully used to predict the proximity of the operating conditions to an impending instability. In the present work, a similar approach is being applied in a pitch-plunge aeroelastic system to provide a quantitative measure to predict the onset of instability. Intermittent bursts obtained in the aeroelastic response are used for recurrence quantification to develop continuous measures capable of forewarning of an impending flutter. Further details regarding recurrence quantification are provided later in Section 4.

3. Experiments

A pitch plunge aeroelastic model of an airfoil is used for the experimental studies carried out in a low speed wind tunnel. The following sections provide details of the experimental set-up, the measurements that were recorded and discussions on the observations.

3.1. The Setup

Wind tunnel experiments were performed on a NACA 0012 airfoil, having a span of 500 mm and a semi-chord length of 50 mm. The position of the elastic axis is located to be at 27% of the chord from its leading edge. It is mounted horizontally in a pitch and plunge setup inside an Eiffel type wind tunnel, at the Bio-mimetics and Dynamics Laboratory, Indian Institute of Technology Madras. The test section is 750 mm in height and 750 mm in

breadth. The fan of the wind tunnel is operated under blowing condition. The maximum mean flow velocity achieved in the empty test section is 25 m/s. A schematic and a photograph of the experimental setup inside the wind tunnel is shown in Fig. 1 and Fig. 2 respectively.

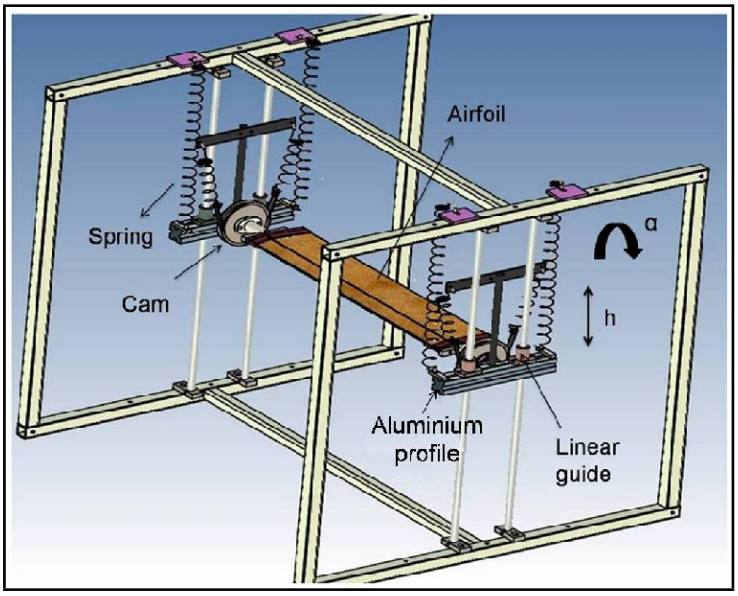

Figure 1: Schematic of the experimental setup

The setup permits two independent degrees-of-freedom for the airfoil motion, namely pitch and plunge movements. The pitching mechanism is similar in design to that provided by O'Neil and Strganac (1998). As shown in Fig. 1, the support structure has two identical translation carriages that are mounted on either side of the test section. The translation carriage on each side comprises of two hardened ground shafts of length 600 mm that pass through a rectangular aluminium profile via linear ball bushing-guide ways. Rigid hooks are attached to the top frame and the aluminium profile, for attaching axial springs. The hooks are threaded with a locknut to re-

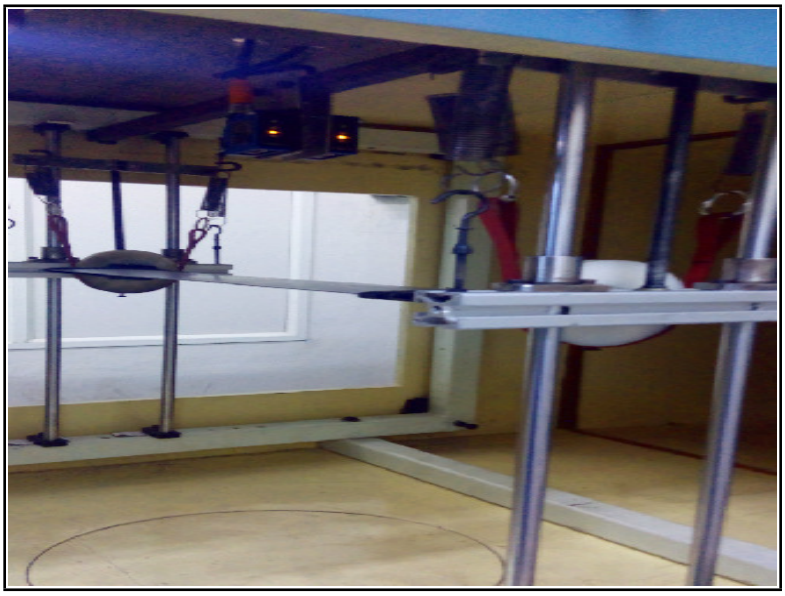

Figure 2: Photograph of the experimental setup

sist loosening of hooks and thereby avoiding free play. To adjust the spring tension and locking, hooks are fitted to the frame and the aluminium profile. The aluminium profile thus keeps the airfoil in suspended condition. The shafts are rigid and fixed to the top and bottom steel frames using adjustable M4-threaded screws. To the aluminium profile, a circular disc of diameter 50 mm and thickness 10 mm is connected via a ball bearing. The disc is made of Nylon to ensure that it is light enough to pitch easily. An industrial Nylon belt having a width of 7.5 mm is circularly enveloped over the disc and fixed with a M3 screw to the bottom of the disc. Rigid hooks are provided here as well to attach the springs that provide restoring forces along the pitching motion. Care is taken to minimize dry friction in the system. A slot is provided in the disc to attach a steel gripper, having a length of 100 mm. The gripper consists of an adjustable steel bar with a hollow pocket

to attach the airfoil into it. Grub screws are used to fix the airfoil firmly into the pocket. The position of the elastic axis is identified by changing the location of the pocket over the adjustable steel bar and tightening the grub screw. The only source of nonlinearity in the structural system arises from the spring stiffness; cubic nonlinear behaviour in the springs were identified in the range of displacements that were encountered. The presence of the set-up with its bars and frame structure inside the tunnel test section introduces turbulence and fluctuations to the free- stream. The tunnel fan is also operated in the blowing condition which further contributes to the fluctuations. These fluctuations added to the mean flow make the resulting wind field look more real-life as likely to be encountered by various engineering aeroelastic systems. However, quantification of these fluctuations could not be carried out within the scope of the present work.

3.2. Measurements

The airfoil has displacements along both the pitch and plunge directions. The displacement measurements along both pitch and plunge are acquired simultaneously using a pair of Wenglor opto NCDT type laser sensors that have a measuring range of 300 mm. A 4-channel ATALON Data Acquisition system having an input voltage of $\pm 5V$ and 24-bit resolution is used to acquire the signals from the laser sensors. Typical duration of sample acquisition for the airfoil response is 40 seconds, with a sampling frequency of 5024 Hz. Use of filter is avoided and the raw data is acquired. The mean angle of attack of the airfoil is set to zero degrees. Initially, static tests are performed to identify the structural parameters of different components of the experimental setup; these are listed in Table 1.

Wind tunnel tests are conducted by systematically varying the mean flow velocity from 3.6 to 7.6 m/s in steps of 0.2 m/s. The mean wind speed measurements have an uncertainty of ± 5 %. A Delta HD 4V3 TS3 air velocity sensor is used to measure the flow velocity. The sensor has a measurement range of 0-40 m/s and a sensitivity of ± 0.1 m/s. The air velocity sensor is connected to the same data acquisition system for recording the flow velocity.

Additionally, a pitot tube manometer is also located at the beginning of the test section to monitor the flow speeds. First, the damping trend is analyzed in pitch and plunge mode by giving an initial disturbance to the airfoil under zero wind velocity condition. The decaying pitch and plunge responses are measured and using the logarithmic decrement technique, the viscous damping ratio in each mode is estimated. Fast Fourier transform (FFT) analysis of the free decay test is used for obtaining ω_y and ω_α and were found to be 4.312 Hz and 4.316 Hz respectively. The bin size for calculating the FFT was 0.00145 Hz.

3.3. Observations and discussions

The experiments were initiated with the flow speed well below the flutter speed and measurements were acquired for the response of the undisturbed airfoil. The airfoil appeared to be at rest for U less than 4 m/s. In this

m_1	m_2	m_3	m_y	m_α	I_α	k_y	k_α	S
1.1	0.9	0.4	2.4	1.3	0.0017	2000	1.25	0.006
Kg	Kg	Kg	Kg	Kg	Kg-m^2	N/m	Nm/rad	Kg-m

Table 1: Physical parameters of the experimental setup.

regime, any initial perturbation given to the pitch-plunge system is observed to eventually die down.

As the wind speed is slowly increased to 4 m/s, the unperturbed airfoil is observed to undergo very low amplitude oscillations. The time histories for the plunge and the pitch on the airfoil are shown respectively in Fig. 3a and Fig. 4a. It can be seen that the oscillations appear "noisy". How-

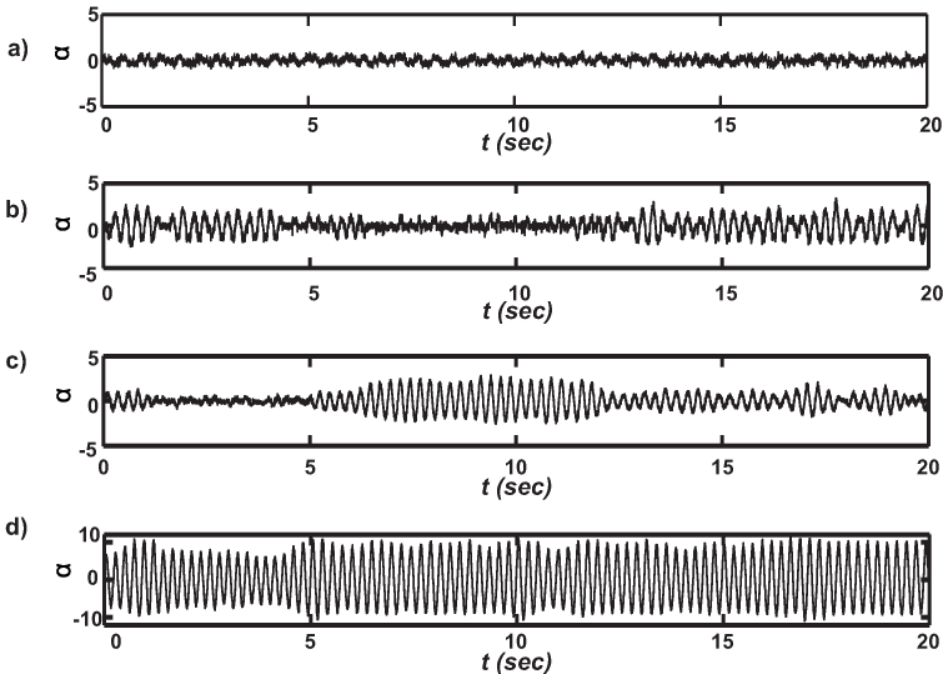

Figure 3: Pitch response, $\alpha(^\circ)$, of airfoil for flow speed a) $U = 4$ m/s, b) $U = 6$ m/s, c) U= 6.6 m/s, and d)U=7.2 m/s.

ever, as the wind speed is increased further, bursts of periodic oscillations are observed; see Fig. 3b & Fig. 4b for the pitch and plunge responses when $U = 6$ m/s. These intermittent burst oscillations are characterized by periodic segments of an uncertain duration followed by segments of comparatively lower amplitude aperiodic fluctuations and then back again to periodic

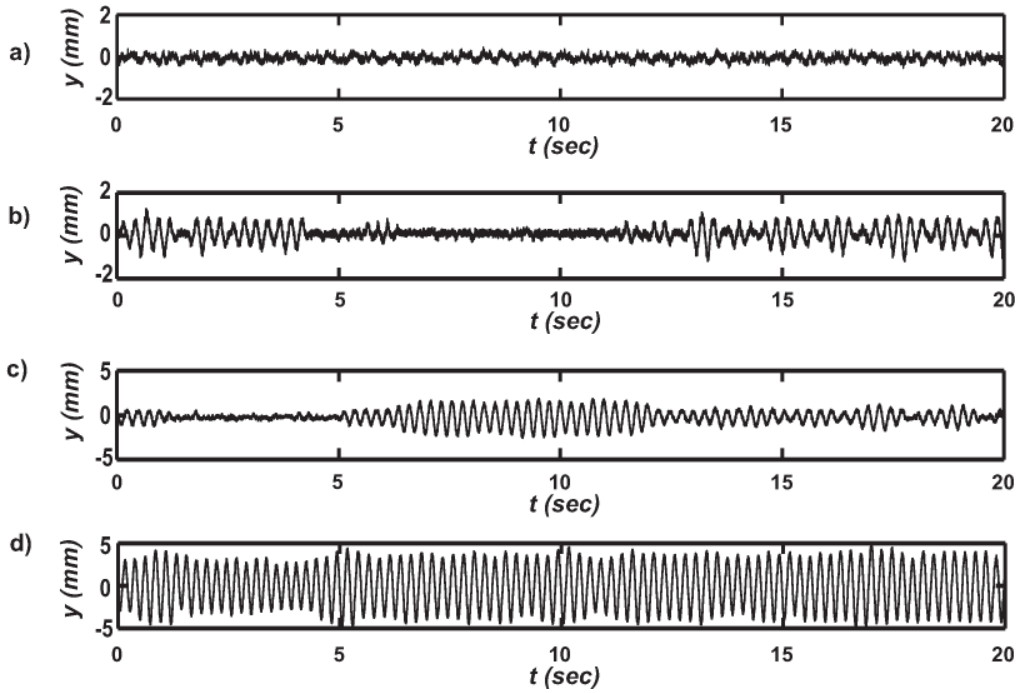

Figure 4: Plunge response, $y(mm)$, of airfoil for flow speed a) $U = 4$ m/s, b) $U = 6$ m/s, c) $U = 6.6$ m/s and d) $U = 7.2$ m/s

.

oscillations. Monitoring the response for longer durations revealed that the observed bursts do not correspond to transients in the dynamics, *i.e.*, the response does not eventually transform itself to periodic oscillations or to a fixed point. Instead, they were observed to persist as the measurement time was increased. This rules out the possibility of mixed type LCOs as was observed by Marsden and Price (2005), which was a transient phenomenon.

On increasing the wind speed further, the duration of intermittent bursts as well as their amplitude were observed to increase significantly; see Fig. 3c and Fig. 4c. Finally, at $U = 7.2$ m/s, the intermittency is lost and the response transitions to a fully developed LCO; see Fig. 3d and Fig. 4d.

We observe that such intermittent bursts always precede LCO in our experiments; here only a few of the observed intermittent responses are reported in Fig. 3 and Fig. 4 for the sake of brevity.

In order to understand the appearance of such intermittent responses in the aeroelastic experiments, the effect of turbulence needs to be taken into account. In a turbulence free system, the onset of flutter, is a transition from a fixed point to a LCO, *i.e.*, a Hopf bifurcation and this scenario leaves no room for the appearance of intermittent burst oscillations of the type observed in our experiments The large variation of the response amplitude requires additional time scales which are much slower than the structural time scale. Typically, turbulent velocity fluctuations have a higher energy content at lower frequencies. Hence, it can be conjectured that the wind fluctuations that operate over a slower time scale can give rise to intermittent bursts by shifting the dynamics of the airfoil back and forth about its Hopf bifurcation point. A numerical study is presented in Section 5 in which a canonical fluctuating wind model on a pitch plunge binary flutter system is able to show the existence of intermittency, qualitatively similar to the results presented in this section.

4. Precursors to Impending Instability

The focus of the present work is to develop quantitative measures (precursors) to forewarn the onset of flutter LCOs from measurement data. From the experimentally obtained time histories, the appearance of instability was always observed to be preceded by a regime of intermittency in both the degrees of freedom. Therefore, a measure that can characterize and quantify

these intermittent states can act as a precursor to an impending flutter. A convenient way to describe such repeating patterns in the dynamics of these bursts can be extracted using a visualization technique known as a recurrence plot which is explained next.

4.1. Recurrence quantification

In deterministic dynamical systems, recurrence is a fundamental property and recurrence plots are useful to visually identify the times at which the trajectory of the system visits approximately the same area in the phase space (Marwan et al., 2007). The use of recurrence plots as a tool for characterizing the temporal features in the dynamics of a measured signal, by tracking the regularity of the trajectories, was first suggested in Eckmann et al. (1987). A recurrence plot is defined as an array of dots in a $N \times N$ square, where a dot is placed at location (i, j), if the proximity between $y(j)$ and $y(i)$ is small. Here, $y(i)$ is the i-th point in a trajectory describing a dynamical system and $y(j)$ is some other point in the trajectory. It is to be noted that a recurrence plot has units of time in both axes. Obtaining recurrence plots requires the reconstruction of the underlying mathematical phase space of evolution of the measured aeroelastic-response fluctuations.

The necessity to reconstruct the phase space of the measured aeroelastic response (in general, any measured time series) arises because usually in a physical experiment, one can measure only a few of the variables of the state space vector. In the aeroleastic experiment carried out in this study, we measure only the displacements along the pitch and plunge; measuring the velocities along these directions is more difficult and expensive. In these situations, phase space reconstruction of the measured time signal helps visualize

the system dynamics at various operating conditions. For instance, a limit cycle would correspond to a closed loop around a fixed point in the reconstructed phase space (Takens, 1985). Also known as delay-embedding, the measured time series is converted into a set of delay vectors that have a one-to-one correspondence with one of the state variables involved in the system dynamics. We construct the vectors $[y(t), y(t+\tau), y(t+2\tau), \ldots, y(t+d-1)\tau]$ from the measured response data $y(t)$ such that these vectors in combination provide the maximum information on the airfoil dynamics. Here 'y' refers only to the plunge degree of freedom; the same can be carried out for pitch response 'α'. The elements of these vectors are the coordinates in the d-dimensional phase space of evolution of the time signal. For instance, $y(d) = [y(t_i), y(t_i+\tau), y(t_i+2\tau), \ldots, y(t_i+d-1)\tau]$ is the point in the d-dimensional phase space at time instant t_i.

To accomplish an appropriate reconstruction, we need to obtain the optimum time lag, τ_{opt}, amongst the delay vectors and the least embedding dimension, d_0, for the phase space composed of these delay vectors such that the dynamics is completely captured. The first minimum of the average mutual information between the delay vectors is estimated as the optimum delay τ_{opt} (Abarbanel et al., 1993). The average mutual information, $I(\tau)$, of a signal $y(t)$ is given by the expression

$$I(\tau) = \sum_{i=1}^{N} P(y(t), y(t+\tau)) \log_2 \left[\frac{P(y(t), y(t+\tau))}{P(y(t)P(y(t+\tau))} \right], \tag{1}$$

where, $P(\cdot)$ denotes the probability of occurrence of an event, t is the measurement time and τ is the time lag.

Further, so as to compute the average mutual information for various

time lags τ, we first normalize the time signal $y(t)$ between 0 and 1. Then the data is sorted in bins, and the probability distributions $y(t)$ and $y(t+\tau)$ are then obtained by normalizing the histograms on these bins. Additionally, the joint probability distribution $P(y(t), y(t+\tau))$ can also be obtained by normalizing a two dimensional histogram obtained in a two dimensional bin in $y(t)$ and $y(t+\tau)$. The average mutual information, which is a function of the time delay between the data points of a time series, is an indicator of the amount of information shared by two sets of data. Therefore, the minimum would correspond to a set of vectors that can provide more information about the system than either of the vectors considered in isolation.

In order to get a suitable embedding dimension d_0, the technique developed by Cao (1997) is used. The methodology is an optimized version of the False Nearest Neighbours (FNNS) method (Abarbanel et al., 1993) and involves tracking the fraction of false neighbors in the phase space as d_0 is continuously changed. In the phase space, a false neighbor continuously changes its relative position with respect to its neighboring points as the value of d_0 keeps increasing. Mathematically, one constructs a measure $a(i,d)$ to track the FNNS as,

$$a(i,d) = \frac{||y_i(d+1) - y_{n(i,d)}(d+1)||}{||y_i(d) - y_{n(i,d)}(d)||}, \tag{2}$$

where, $i = 1, 2, ..., (N - d\tau)$ and $n(i,d)$ is the index of the nearest neighbouring point in the phase space to the point y. Here, $||\cdot||$ is the second norm and represents the Euclidean distance between two points. The dependency on the index i is removed by taking the average $a(i,d)$ obtained at different

values of i as

$$E(d) = \frac{1}{N - d\tau_{opt}} \sum_{i=1}^{n-d\tau} a(i,d). \tag{3}$$

Note that $E(d)$ depends only on the dimension d and τ_{opt}. The variation of $E(d)$ on increasing the dimension from d to $d+1$ is determined by defining $E_1(d)$ as

$$E_1(d) = \frac{E(d+1)}{E(d)}. \tag{4}$$

Once the value of d is greater than d_0, the value of $E_1(d)$ stops changing and d_0 is selected to be the minimum embedding dimension for the chosen time series. Quite often, it is difficult to distinguish a stochastic signal from a deterministic signal by merely observing the variation of $E_1(d)$ for various values of d. While $E_1(d)$ saturates beyond a certain value of d for a deterministic signal, it always increases with increasing d for a stochastic signal. Hence, to distinguish a deterministic signal from a stochastic one, an additional measure $E_2(d)$ is defined (Cao, 1997; Nair et al., 2013) as

$$E_2(d) = \frac{E^*(d+1)}{E^*(d)}, \tag{5}$$

where,

$$E^*(d) = \frac{1}{N - d\tau_{opt}} \sum_{i=1}^{n-d\tau} |y(i + d\tau_{opt}) - y(n(i,d)) + d\tau_{opt}|. \tag{6}$$

Since for a stochastic signal, the future values are independent of past values, $E_2(d)$ is independent of d and is equal to 1 for all values of d. Whereas, for a deterministic signal $E_2(d)$ depends on d, there must be some values of d for which $E_2(d)$ is not equal to 1.

The average mutual information and the measures to obtain embedding dimension of the responses at various wind speeds are given in Fig. 5. We

see the data at $U = 4$ is stochastic as $E_2(d) = 1$ for all values of d. The embedding dimension d_0 of the phase space shows no significant variation after $d = 10$ for all the signals. Thus, the optimum dimension was chosen to be 10 and the embedding delay was estimated from the first minimum of $I(\tau)$ ($\tau_{opt} = 62.5$ ms in this case).

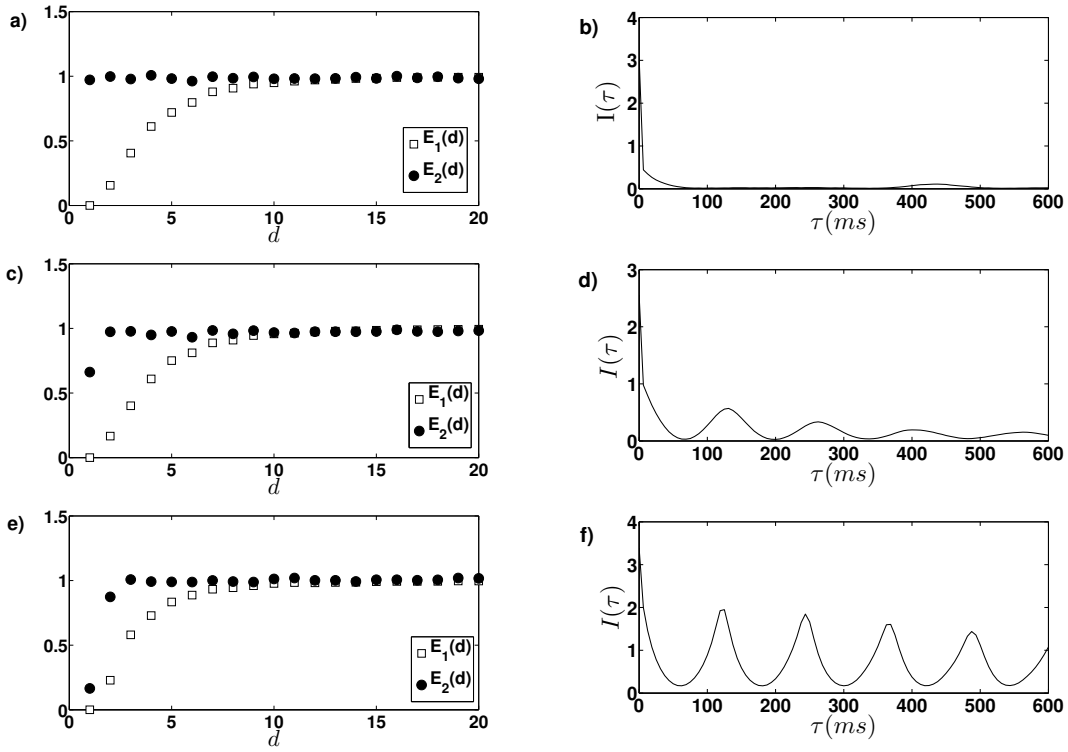

Figure 5: The values of $E_1(d)$ and $E_2(d)$ for the measured data are shown at a) $U = 4$ m/s, c) $U = 6$ m/s and e) $U = 7.2$ m/s. All the three cases shows that $E_1(d)$ and $E_2(d)$ saturates for $d = 10$. Similarly, the average mutual information for the three different wind speeds are shown in b), d) and f). The optimum time delay for embedding was estimated from the first minimum of average mutual information I.

Once the phase space is reconstructed, recurrence plots are constructed by estimating the pairwise distances between points in the phase space. This

creates a binary recurrence matrix R_{ij}, defined as

$$R_{ij} = \Theta(\epsilon - \parallel y_i - y_j \parallel), i, j = 1, 2, ..., N - d_0\tau_{opt}, \tag{7}$$

where, Θ is the Heaviside function and ϵ is the upper limit of the distance between a pair of points in the phase space to consider them as 'close' or 'recurrent'. The indices represent the various time instances when the distances are computed. Being a symmetric matrix comprising of zeros and ones, the recurrence matrix can be represented in a 2D form as a recurrence plot, as the trajectories evolve with time. The 'ones' correspond to black points and represent those time instants when the pairwise distance are less than the threshold ϵ, while the 'zeros' in the recurrence plot are marked white and correspond to those instants when the pairwise distances exceed ϵ. An important parameter in constructing a recurrence plot is ϵ. If ϵ is too small then there might not be any recurrence points and hence nothing can be said about the underlying dynamical system. On the contrary, if a large threshold is chosen, then almost every point is selected to be in the neighbourhood of each other (Marwan et al., 2007).

In constructing the recurrence plots, a two-pronged approach was followed. For the purpose of visualization, the threshold ϵ was selected as a relative measure that depends on the size of the attractor at that particular operating condition (in this case, the flow speed). This enables one to understand the qualitative changes in the underlying dynamics in phase space. On the other hand, in order to obtain quantifiable precursors across different values of flow velocities, the threshold was held fixed at some suitable value. Fixing the threshold allows one to compare the values of the various statistical measures obtained using recurrence quantification as the

control parameter is varied. The fixed threshold value (say ϵ) was chosen to be slightly higher than the size of the attractor obtained at the lowest operational velocity. It should be mentioned that the sizes of the thresholds are indicative of the Euclidean distances between points in the phase space ($\sqrt{d_0} \mid y \mid$), and should not be confused with the amplitude levels of the airfoil ($|y|$).

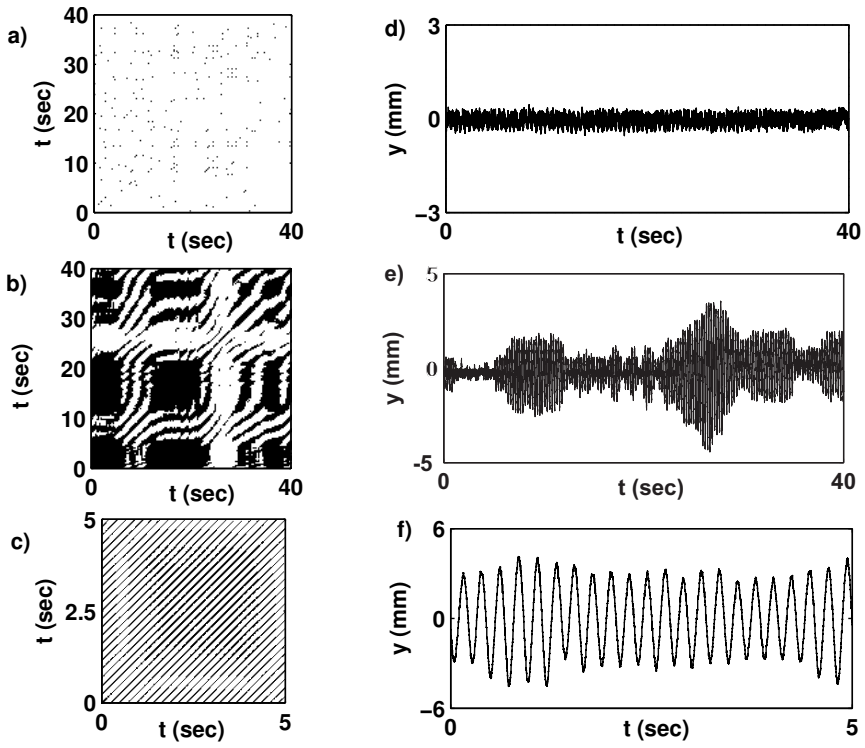

Figure 6: Recurrence plots and the respective plunge response measurements acquired during wind tunnel tests carried out for $U = 4$ m/s (top row), $U = 6.6$ m/s (middle row) and $U = 7.2$ m/s (bottom row). The black patches in the intermittent response seen in (b) corresponds to regions of low amplitude response fluctuations relative to chosen threshold. The recurrence plot in (c) develops into clear diagonal lines at instability. Note that the distance between the diagonal lines in (c) gives the time period of oscillation during LCO.

The recurrence plots obtained for the measured aeroelastic plunge response is shown in Fig. 6. Note that here the recurrence plot for the pitch response is not shown for the sake of brevity; however the characteristic features are observed to be similar. The data was under sampled to a frequency $F_s = 160$ Hz. The data was under sampled to reduce the computation involved in obtaining the recurrence plots. For $U = 4$ m/s, the response consists of noisy, low-amplitude fluctuations and hence the recurrence plot appears grainy; see Fig. 6a and Fig. 6d. Figure 6b shows the recurrence plot for the intermittent signal that precedes instability, when $U = 6.6$ m/s. A mixture of perforated black patches amidst white patches are seen. As mentioned earlier, the black patches correspond to the time spent by the system in low amplitude chaotic fluctuations and the white patches correspond to bursts of periodic oscillations. Since, the response comprises of high amplitude bursts amidst an aperiodic and low amplitude regime, the recurrence plot helps in identifying visually the presence of intermittency in the system. The corresponding intermittent time response, in heave, is shown in Fig. 6e.

As the flow speed is further increased, the airfoil starts undergoing LCO. The recurrence plot for this situation can be seen in Fig. 6c. Now, the recurrence plot is observed to have a pattern of diagonal lines, indicating high repeatability, or rather recurrence, in the response dynamics. Here, the duration of signal was chosen to be only 5 seconds, so that the diagonal lines are clearly visible. By measuring the distance between the diagonal lines, the fundamental period of oscillation during aeroelastic instability can be obtained. The corresponding time history of the signal is shown in Fig. 6f which is observed to constitute modulated limit cycle oscillations. The

recurrence plots in Fig. 6 help in visually understanding the transition from intermittency to instability in the aeroelastic system.

4.2. Statistical measures

Once the recurrence plot has been constructed, a number of statistical measures can be obtained, by tracking the probability distribution of black points (or white points) in such plots. These measures can serve as precursors to an impending aeroelastic-flutter. Similar measures have been developed in the context of obtaining precursors to combustion instability in Nair et al. (2014). A decrease in the density of black points corresponds to a dip in the time spent by the system in aperiodic states which is characterized by a quantity τ_0, defined as,

$$\tau_0 = \frac{1}{N_1} \frac{\sum_{v=1}^{N_1} vY(v)}{\sum_{v=1}^{N_1} Y(v)}. \tag{8}$$

Here, $N_1 = N - d_0\tau_{opt}$, $Y(v)$ is the frequency distribution of the vertical (horizontal) black lines of length v in the recurrence plot for a signal sampled at a frequency F_s. Also, τ_0 quantifies the duration for which a system remains in a particular dynamical state; in the current problem this is the aperiodic fluctuations. Therefore, it is expected that the quantity τ_0 approaches zero as the systems transforms itself into a LCO as seen in Figs 7b.

Another measure that can be constructed from the recurrence plots is the Shannon entropy. The Shannon entropy of the signal can be obtained from the recurrence plot using the expression

$$s = -\sum_{l=1}^{N_1} P(l) \ln(P(l)), \tag{9}$$

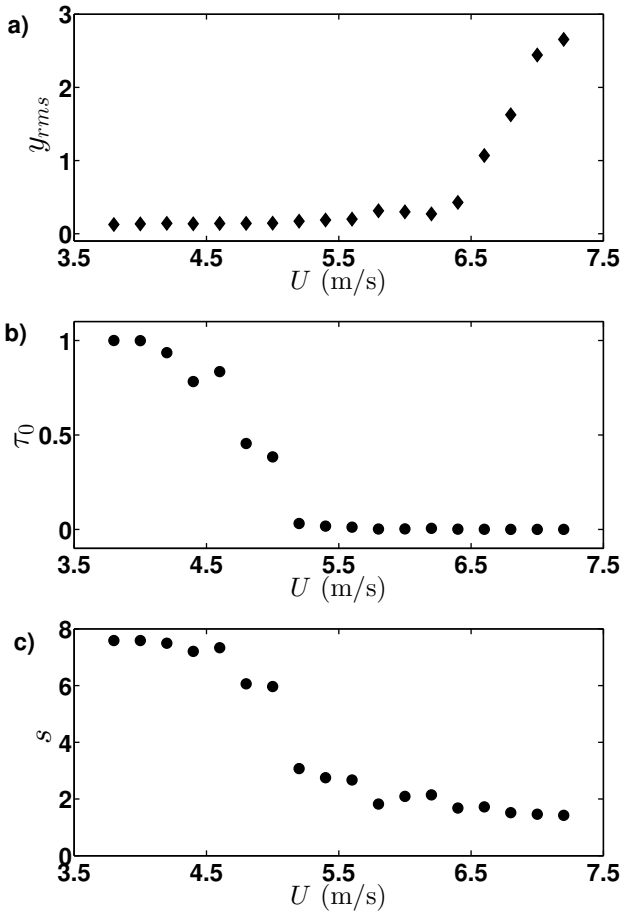

Figure 7: Statistical measures constructed from recurrence quantification of the aeroelastic response; a) variation of r.m.s of response as flow speed is changed; b) average passage time spent by the response in aperiodic fluctuations; c) computed Shannon entropy of the diagonal length distribution in recurrence plot. Clearly, the r.m.s value of the response undergoes a significant rise only as we approach aeroelastic instability (past $U = 6.5$ m/s). Statistical measures on the contrary start showing a decrease well in advance of flutter, i.e., from the intermittent regime itself, a drop in the values of trapping time and Shannon entropy is evident from b) and c).

where, $P(l)$ is the probability that a diagonal line has length l, and is given by

$$P(l) = \frac{Y(l)}{\sum_{l=1}^{N_1} Y(l)}. \tag{10}$$

Here, $Y(l)$ is the frequency distribution of the vertical (horizontal) black lines of length l in the recurrence plot. A gradual decrease in entropy implies that the system is approaching a state of regularity or there is an emergence of order from chaos. This is expected, since we are aware that recurrence plots for a periodic signal consists of black, parallel and diagonal lines and that the oscillations correspond to an ordered state. Hence, it is natural to expect a drop in entropy as the system approaches instability; see Fig. 7c. In Fig. 7a, the variation of r.m.s. of the measured response with rise in wind speed is shown. Note that an appreciable change in the r.m.s. of the response is observed much later at around 6.6 m/s - values at which the other two measures have already stabilized. This implies that y_{rms} changes much closer to the LCO region and cannot be used as effectively as a precursor like the other two measures. On the contrary, the precursors developed based on recurrence quantification indicates the onset of flutter well ahead of the instability regime. For instance, the value of τ_0 is seen to decrease when $U = 4.5$ m/s. Similarly, the Shannon entropy, s, decreases as U goes beyond 4.5 m/s. Clearly, these measures can foretell the change in dynamics of the system well in advance.

4.3. Model independence

It must be reemphasized here that the precursors developed here are model independent. A model free method to predict instabilities has distinct

practical advantages over a model dependent approach. A primary difficulty with model based approaches to predicting the stability boundary lies in developing an accurate mathematical model for the system. Any uncertainties in developing the model propagate through the analysis and leads to predictions of the stability boundaries, which are itself uncertain. Additionally, due to the effect of ageing, the structural parameters usually degrade with time. This leads to changing of the stability boundaries with time. Unfortunately, mathematical models for ageing of structural components are not as well developed and hence significant epistemic uncertainties are introduced into the formulation when ageing effects are incorporated into the mathematical model. In real life applications, it is expected that both these uncertainties exist. For assessment of the stability boundaries using model dependent techniques, therefore, require accurate identification of the system parameters of the mathematical model. Hence, solving an inverse problem and carrying out model updating is an essential step in model based approaches. This is not only time consuming but is expensive as well, requiring significant investments in measurements as well as computations. On the other hand, the precursors developed here requires only continuous measurements of the airfoil response. In a generic sense, these measures only distinguish the passage of dynamics from an irregular state to a periodic one through intermittency. Therefore, such precursors can possibly be used as early warning signals to an impending instability in a variety of turbulent flow systems encountering periodic oscillations, without the need for developing mathematical models for the aeroelastic system.

5. Numerical Investigations

Though the advantage of the proposed precursors is their effectiveness in predicting the onset of flutter instability even without the necessity of mathematically modelling the system, questions persist on the accuracy of the proposed framework in identifying the flutter boundary. An answer to these questions can be obtained by carrying out a numerical analysis on an equivalent mathematical model for the pitch-plunge system. This section therefore focusses on carrying out investigations on a numerical pitch-plunge model of an airfoil to demonstrate that the precursors developed in this paper can indeed be used for predicting the onset of flutter instability.

The numerical investigations are carried out using a well known mathematical model for a pitch-plunge oscillating airfoil, available in Fung (1955); Lee and Jiang (1999). However, some modifications are in order as the contribution of mass from the experimental set-up along the pitch and plunge modes are different. The mass of the translation carriage do not take part along the pitching degree of freedom and this requires a suitable modification in the equations of motion. The total mass of the system is divided into three parts: m_1 is the additional mass in plunge corresponding to the frame, m_2 is the mass the pitching mechanism and m_3 is the mass of the airfoil having its centre of mass at a distance bx_α behind the elastic axis, where x_α is the nondimensional distance from the elastic axis to the airfoil centre of mass. These components are shown in the schematic diagram of the airfoil presented in Fig. 8.

The total moving mass in plunge is $m_y = m_1 + m_2 + m_3$. The moment of inertia about elastic axis is I_α is computed based on the total moving mass

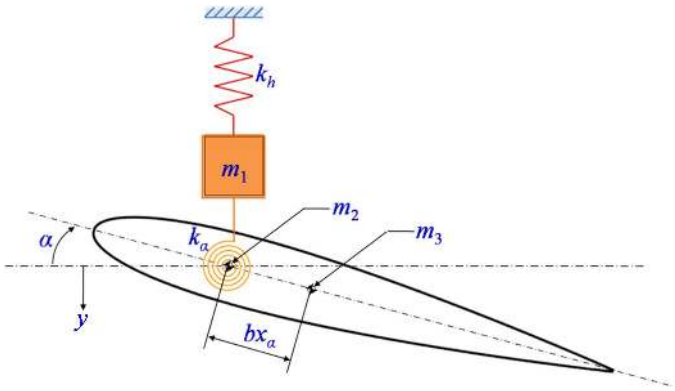

Figure 8: Schematic of airfoil section model

in pitch given by $m_\alpha = m_2 + m_3$. Following the formulation in Marsden and Price (2007), it can be shown that the equations of motion can now be expressed as

$$m_y\ddot{y} + m_3 b x_\alpha \ddot{\alpha} + k_y y + L = 0, \tag{11}$$

$$m_3 b x_\alpha \ddot{y} + I_\alpha \ddot{\alpha} + k_\alpha \alpha - L(0.5 + a_h)b = 0. \tag{12}$$

Here, for steady flow conditions,

$$L = 2\pi\rho U^2 b\alpha, \tag{13}$$

and for quasi-steady flow conditions,

$$L = 2\pi\rho b U^2 \Big(\alpha + \frac{\dot{y}}{U} + (0.5 - a_h)\frac{b\dot{\alpha}}{U}\Big). \tag{14}$$

Note that in accordance with the thin airfoil theory, the lift slope is taken to be 2π. Using the notation for the uncoupled natural frequencies as $\omega_y = k_y/m_y$ and $\omega_\alpha = k_\alpha/I_\alpha$, and a nondimensional frequency parameter $p = \nu b/U$ with ν as the flutter frequency, an eigenvalue form can be obtained. The other

nondimensional parameters are (see the Nomenclature for description): $r^2 = I_\alpha/m_\alpha b^2$, $\varpi = \omega_y/\omega_\alpha$, $\mu = m_y/\pi\rho b^2$ and $V = U/b\omega_\alpha$, where $y = \bar{y}\exp(\nu t)$ and $\alpha = \bar{\alpha}\exp(\nu t)$. The eigenvalue problem for the steady flow conditions can be expressed as

$$\begin{bmatrix} p^2 + \frac{\varpi^2}{V^2} & \frac{m_3}{m_y}x_\alpha p^2 + \frac{2}{\mu} \\ \frac{m_3}{m_y}x_\alpha p^2 & \frac{m_\alpha}{m_y}r^2p^2 + \frac{m_\alpha}{m_y}\frac{r^2}{V^2} - \frac{2}{\mu}(a_h + 0.5) \end{bmatrix} \begin{Bmatrix} \frac{\bar{y}}{b} \\ \bar{\alpha} \end{Bmatrix} = \begin{Bmatrix} 0 \\ 0 \end{Bmatrix}. \tag{15}$$

The corresponding eigenvalue problem for the quasi-steady flow conditions is expressed as

$$[A] \begin{Bmatrix} \frac{\bar{y}}{b} \\ \bar{\alpha} \end{Bmatrix} = \begin{Bmatrix} 0 \\ 0 \end{Bmatrix}. \tag{16}$$

where the matrix $[A]$ is a 2×2 matrix of the form

$$\begin{bmatrix} p^2 + \frac{2p}{\mu} + \frac{\varpi^2}{V^2} & \frac{m_3}{m_y}x_\alpha p^2 + \frac{2p}{\mu}(0.5 - a_h) + \frac{2}{\mu} \\ \frac{m_3}{m_y}x_\alpha p^2 - \frac{2p}{\mu}(a_h + 0.5) & \frac{m_\alpha}{m_y}r^2p^2 - \frac{2p}{\mu}(a_h + 0.5)(0.5 - a_h) + \frac{m_\alpha}{m_y}\frac{r^2}{V^2} - \frac{2}{\mu}(a_h + 0.5) \end{bmatrix}. \tag{17}$$

The eigenvalues obtained from Eqs.(15-16) typically constitute a complex conjugate pair of roots of the form

$$\begin{aligned} p_1 &= \Gamma_1 \pm \mathrm{i}\Omega_1, \\ p_2 &= \Gamma_2 \pm \mathrm{i}\Omega_2. \end{aligned} \tag{18}$$

The behaviour of these complex roots with wind speed (U) can be used to verify the onset of flutter instability (Dowell et al., 1995). Figure 9 shows the variation of the real and imaginary components of these eigenvalues, for both the steady and the quasi-steady cases. In steady flow condition, the onset of flutter is identified by the coalescence of the imaginary components of the eigenvalues (dashed lines corresponding to the imaginary components

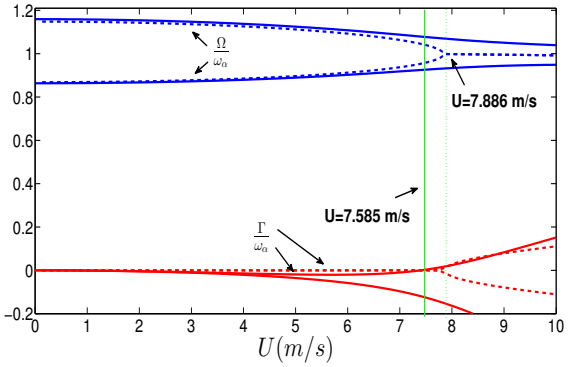

Figure 9: Variation of real (modal damping) and imaginary parts (modal frequency) of solution of Eqs. 15 and 16 with airspeed. The dashed lines correspond to steady aerodynamics and the solid ones correspond to quasi steady aerodynamics.

of the eigenvalues) and is seen to occur at $U = 7.9$ m/s. When the flow is quasi-steady, the onset of flutter is characterized as when the modal damping, denoted by the real part of the eigenvalues, changes from zero to a positive value indicating divergence and is seen to occur at $U = 7.6$ m/s; see the full line corresponding to the real components of the eigenvalues. More details on the theory behind this is available in Dowell et al. (1995) and is not repeated here.

In the case of unsteady aerodynamic modelling, the loads are expressed in terms of the following integro-differential form (Fung, 1955),

$$\begin{aligned} L(t) &= 2\pi\rho bU^2[\alpha(0) + \frac{\dot{y}(0)}{U} + \frac{b}{U}(0.5 - a_h)\dot{\alpha}(0)]\phi(t) \\ &\quad +2\pi\rho bU^2 \int_0^t \phi(t - t_0)[\dot{\alpha}(t) + \frac{\ddot{y}(t)}{U} + \frac{b}{U}(0.5 - a_h)\ddot{\alpha}(t)]\mathrm{d}t_0. \quad (19) \end{aligned}$$

The time function $\phi(\tau)$ is the Wagner's function which can be approximated as (Jones, 1958)

$$\phi(\tau) = 1 - 0.165\exp(-0.0455\tau) - 0.335\exp(-0.3\tau). \quad (20)$$

The integro-differential equations are numerically integrated following the procedure adopted in Lee and Jiang (1999). From the bifurcation diagram obtained numerically and shown in Fig. 10, it can be seen that the onset of LCO occurs at $U = 7.5$ m/s via a supercritical Hopf bifurcation. The physical

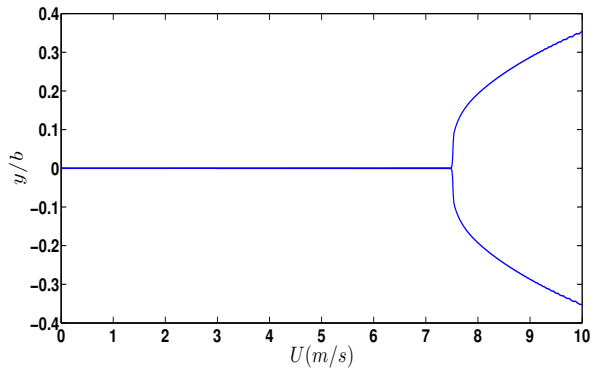

Figure 10: Bifurcation diagram of the response as a function of U.

parameters estimated from the experimental set-up were given in Table 1; the corresponding nondimensional values used here for the numerical analysis are listed in Table 2. Note that the onset of LCO observed in the experiments was approximately $U = 7.2$ m/s. However, as has been mentioned earlier in Section 3, the flow in the wind tunnel was not uniform but was accompanied by fluctuations.

So far in the numerical calculations, the flow has been assumed to be

r	μ	x_α	ζ_α	ζ_y	ϖ
0.707	660	0.29	0.03	0.05	0.999

Table 2: Non-dimensional parameters of the experimental setup

uniform and without any fluctuations. In such sterile conditions, the intermittent behaviour that has been observed in the experiments cannot be seen. To numerically investigate intermittency in the presence of fluctuations, a simple canonical model for the flow fluctuations is assumed. The uniform flow is superimposed with a sinusoidal component whose frequency of oscillation is assumed to have variations with time about a dominant frequency. This is a simple artifice to capture the disturbed flow-field in terms of a dominant frequency with perturbations in the absence of a precise quantification of the actual fluctuations using sophisticated hardwares like LDV or PIV. Thus, the non-dimensional flow speed V is now taken as

$$V = \frac{U_m}{b\omega_\alpha}(1 + a\sin(\omega_r t)), \tag{21}$$

where, U_m is the dimensional mean wind speed in m/s, a indicates the amplitude of the fluctuating component and is taken to be of $\mathcal{O}(1)$ and ω_r is the frequency of the sinusoid, adjusted such that, $\omega_r = \omega_0 + \kappa R$. Here, κ is a constant of $\mathcal{O}(\omega_0)$ and R is a uniformly distributed random variable in $[0, 1]$ (randomly varies in time). This model is adopted such that random perturbations are added in time to a dominant frequency component in the assumed sinusoidal form. It must be stressed here that this simplistic model cannot represent the secondary structures and is not an actual representation of the flow-field in the wind tunnel.

The time histories of the plunge response non-dimensionalized by semi-chord, for various wind speeds are obtained by numerical integration and are shown in Fig. 11. Here, only a few representative responses are shown for the sake of brevity. As U_m is gradually increased, sporadic bursts are observed; see Fig. 11(a)-(c). This intermittency behaviour is qualitatively similar to

the observations from wind tunnel experiments. Finally, well developed LCO are obtained on further increasing U_m; see Fig. 11(d).

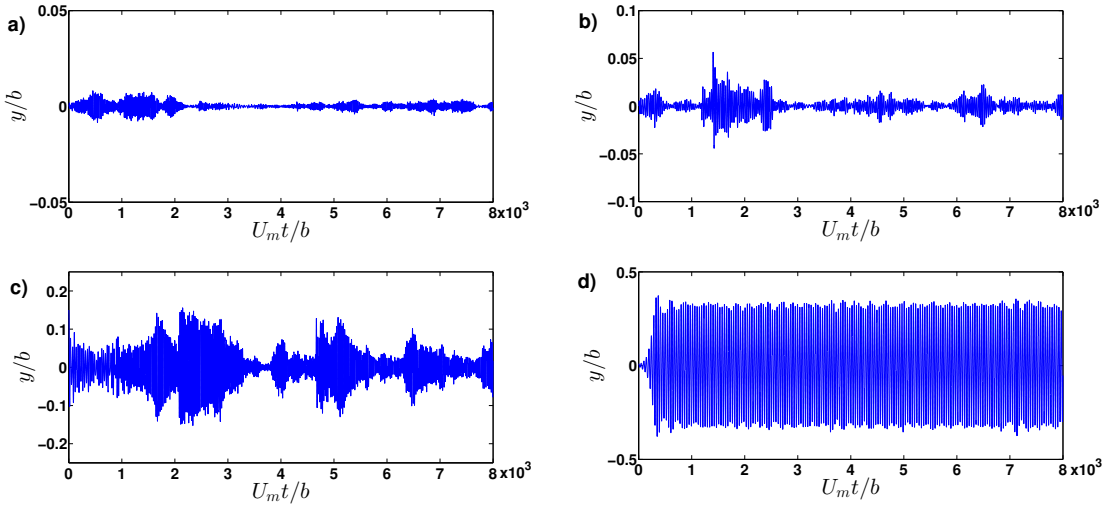

Figure 11: Non-dimensionalized plunge response from numerical model; a) $U_m = 4$ m/s, b) $U_m = 5.2$ m/s, c) $U_m = 6$ m/s and d)$U_m = 7.2$ m/s.

To check the robustness of the precursors proposed in this paper, these synthetically generated time histories are next used to forecast an impending aeroelastic flutter using the proposed recurrence quantification methodology. The optimum embedding dimension (d_0) for the numerical data was computed to be 4 and the embedding delay (τ_{opt}) was chosen to be 149 ms. Figures 12(b) and (c) show the variations of trapping time and Shannon entropy with mean wind speed U_m. The variation of the response r.m.s. is plotted in Figure 12(a). Note that the precursors start decreasing from $U_m = 4.5$ m/s much ahead of the onset of LCOs, obtained at 7.5 m/s in the sterile conditions. Hence they can provide an effective early warning framework. The numerical investigations presented in this section therefore

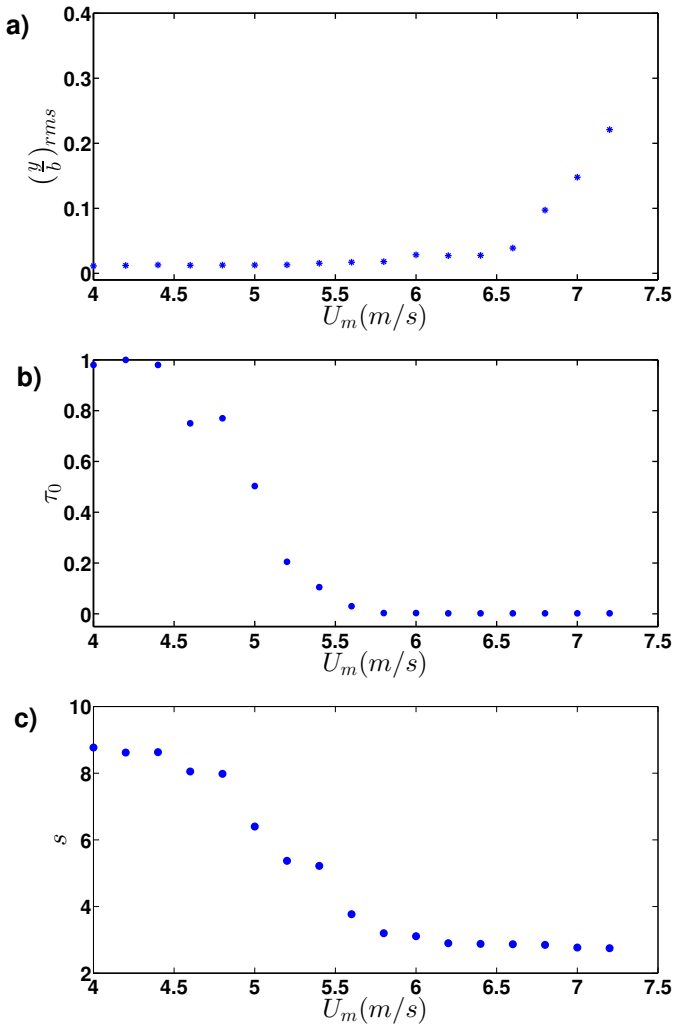

Figure 12: Statistical measures constructed from recurrence quantification of the aeroelastic response obtained numerically; a) variation of r.m.s of response as flow speed is changed. b) average passage time spent by the response in aperiodic fluctuations; c) computed Shannon entropy of the diagonal length distribution in recurrence plot.

provides a qualitative validation to the observations obtained from the wind tunnel experiments. Importantly, the numerical investigations confirm that the precursors proposed in this study are effective in providing an early warn-

ing to the onset of aero-elastic flutter in the presence of flows with fluctuating components. The necessity for the flow to have fluctuations is not unrealistic as in field conditions, the flow will not be sterile due to the interactions with the structure and its various components.

However, the numerical gust model is artificial (as gust quantification is not part of this work) and is only considered to bring out the intermittency in the numerical pitch-plunge model. The objective of this numerical exercise is to establish a qualitative similarity to the experimental observations. This artificial model does not attempt to mimic the actual turbulent condition in the tunnel. On the other hand, quantifying the turbulent wind condition in the tunnel and estimating its COV would be very interesting and provide a realistic measure of the turbulent intensity. This can be taken up in the future.

6. Concluding Remarks

Based on the studies carried out to investigate the intermittent bursts in the aeroelastic response, the following conclusions emerge:

1. The transitions in response from an equilibrium state to aeroelastic flutter in an airfoil under turbulent flow environment is seen to be presaged by an intermittent regime composed of bursts of high amplitude periodic oscillations amidst regions of aperiodic, low-amplitude fluctuations. This gives an altogether different picture from what one would expect from a mean-field description of the phenomenon, wherein the transition happens from a fixed point to a limit cycle via a Hopf bifurcation. To the best of the authors' knowledge, though such intermittency

behaviour has been observed in aeroelastic literature, they have not been studied.

2. The intermittency observed in the response of aeroelastic systems can be used to develop effective measures that can forewarn of impending flutter based on the principles of recurrence quantification. These measures can be useful to the community in developing effective control measures to prevent the system transgressing to the LCO regime and experiencing large amplitude sustained oscillations. Though extensive literature is available on studies on nonlinear aeroelastic responses, at present there appears to be no reliable measures to pre-determine the onset of instability in airfoils subjected to turbulent flow.
3. The precursor measures described in this paper are observed to detect and forewarn the onset of an oscillatory regime based on measurements taken from the pre-flutter regime. These measures are based on quantifying the intermittency in measured signals, and are effective in a regime which is still some way off from the flutter point. In comparison, existing methods that are available in the literature which forewarn of an impending instability are based on monitoring of structural parameters (like damping) or features of the flow parameters (like dynamic pressure) which change appreciably only in the immediate vicinity of flutter. Hence, these methods fall under a different class of tools complementary to what is proposed here. The method proposed here warns the operator that oscillations are about to set in for further variations in an operating parameter. Having gained this knowledge, the decision lies with the operator whether to avoid the operating conditions

cross over to the regimes of limit cycle operation. Hence, based on the requirement of the user, an appropriate safety margin could be drawn from the developed precursors in the intermittency regime.

4. The novelty of the developed precursors lies in its complete model independence and relies only on measurements. Hence, one need not account for modelling uncertainty and model parameter degradation due to ageing or wear and tear. Importantly, the accuracy of model based approaches lie in accurate identification of the system parameters. This implies the need for the solution of an inverse problem at periodic intervals where the system parameters (which could change with time) are identified from measurement data. For large ordered systems, especially those with nonlinearities, this is not a trivial task. Thus the proposed model free approach eliminates the necessity for system identification and the effects of ageing by directly using the measurement data.

In closing, it needs to be reiterated that the present experimental set-up and the tunnel running conditions contributed to the turbulence needed to generate the intermittent bursts observed in the presence study. The presence of turbulence is of significance, since realistic wind flows are turbulent in nature and a mean flow depiction may be inadequate to carry out a stability analysis under realistic conditions. More studies to gain insights into the behaviour of aeroelastic systems in fluctuating flows is currently being pursued in the group.

References

Abarbanel, H. D. I., Brown, R., Sidorowich, J. J., Tsimring, L., 1993. The analysis of observed chaotic data in physical systems. Reviews in Modern Physics 65, 1331–1392.

Abdelkefi, A., Vasconcellos, R., Marques, F., Hajj, M., 2012. Modeling and identification of free play nonlinearity. Journal of Sound and Vibrations 331, 1898–1907.

Alighanbari, H., Price, S. J., 1996. The post-hopf-bifurcation response of an airfoil in incompressible two-dimensional flow. Nonlinear Dynamics 10, 381–400.

Andrianne, T., Dimitriadis, G., 2011. Experimental analysis of the bifurcation behavior of a bridge deck undergoing across-wind galloping. In: Proceedings of the 8th International Conference on Structural Dynamics, EURODYN, Leuven Belgium. ISBN 978-90-760-1931-4.

Bauer, M., Habip, S., He, D. R., Martienssen, W., 1992. New type of intermittency in discontinuous maps. Physical Review Letters 68, 1625–1628.

Cao, L., 1997. Practical method for determining the minimum embedding dimension of a scalar time series. Physica D 110, 43–50.

Covas, E., Tavakol, R., Ashwin, P., Tworkowski, A., Brooke, J., 2001. In and out intermittency in partial differential equation and ordinary differential equation models. Chaos 11, 404–409.

Cox, D., Curtiss, H. C. J., Edwards, J. W., Hall, K. C., Peters, D. A., Scanlan, R. H., Simiu, E., Sisto, F., 2006. A Modern Course in Aeroelasticity. Springer Science, USA.

Dowell, E., Tang, D., 2002. Nonlinear aeroelasticity and unsteady aerodynamics. AIAA Journal 40, 1697–707.

Dowell, E. H., Crawley, E. E., Curtiss Jr, H. C., Peters, D. A., Scanlan, R. H., Sisto, F., 1995. A Modern Course in Aeroelasticity. Kluwer Academic Publishers, Dordrecht.

Eckmann, J., Oliffson Kamphorst, S., Ruelle, D., 1987. Recurrence plots of dynamical systems. Europhysics Letters 4 (9), 973–977.

Fung, Y., 1955. An Introduction to the Theory of Aeroelasticity. Wiley, New York.

Grebogi, C., Ott, E., Romeiras, F., Yorke, J. A., 1987. Critical exponents for crisis-induced intermittency. Physical Review-A 36, 5365–5380.

Jegadeesan, V., Sujith, R., 2013. Experimental investigating of noise induced triggering in thermoacoustic systems. Proceedings of the Combustion Institute 34, 3175–3183.

Jones, W. P., 1958. Summary of formulae and notations used in two dimensional derivative theory. Tech. rep., British aeronautical research committee, report and memorandum.

Kabiraj, L., Sujith, R., 2012. Nonlinear self-excited thermoacoustic oscilla-

tions: intermittency and flame blowout. Journal of Fluid Mechanics 713, 376–397.

Kehoe, M., 1985. A Historical overview of Flight Flutter Testing. NASA TM-4270.

Korbahti, B., Kagambage, E., Andrianne, T., Razak, N., Dimitriadis, G., 2011. Subcritical, nontypical and period-doubling bifurcations of a delta wing in a low speed wind tunnel. Journal of Fluids and Structures 27, 408–426.

Lee, B., Price, S., Wong, Y., 1999. Nonlinear aeroelastic analysis of airfoils: bifurcations and chaos. Progress in Aerospace Sciences 35, 205–334.

Lee, B. H. K., Jiang, L., 1999. Flutter of an airfoil with cubic restoring force. Journal of Fluids and Structures 13, 75–101.

Lind, R., Brenner, M., 2000. Flutterometer : An on-line tool to predict robust flutter margins. Journal of Aircraft 37 (6).

Lobitz, D. W., 2004. Aeroelastic stability predictions for a mw-sized blade. Wind Energy 7 (3), 211 –224.

Marsden, C., Price, S., 2005. The aeroelastic response of a wing section with structural free play nonlinearity:an experimental investigation. Journal of Fluids and Structures 21, 257–276.

Marsden, C. C., Price, S. J., 2007. Transient and limit cycle simulation of a nonlinear aeroelastic system. Journal of Aircraft 44, 60–70.

Marwan, N., Romano, M. C., Thiel, M., Kurths, J., 2007. Recurrence plots for the analysis of complex systems. Physics Reports 438, 237–329.

Matsuzaki, Y., 2011. An overview of flutter prediction in tests based on stability criteria in discrete time domain. International Journal of Aeronautical and Space Sciences 12 (4), 305–317.

Nair, V., Thampi, G., Karuppusamy, S., Gopalan, S., Sujith, R. I., 2013. Loss of chaos in combustion noise as a precursor of impending combustion instability. International Journal of Spray and Combustion Dynamics 5, 273–290.

Nair, V., Thampi, G., Sujith, R. I., 2014. Intermittency route to thermoacoustic instability in turbulent combustors. Journal of Fluid Mechanics 756, 470–487.

O'Neil, T., Strganac, T., 1998. Aeroelastic response of a rigid wing supported by nonlinear springs. Journal of Aircraft 35, 616–622.

Ott, E., Sommerer, J., 1994. Blowout bifurcations: the occurrence of riddled basins and on-off intermittency. Physics Letters-A 188, 39–47.

Poirel, D., 2001. Random Dynamics of a Structurally Nonlinear Airfoil in Turbulent Flow. Department of Mechanical Engineering, McGill University, Canada.

Poirel, D., Dunn, S., Porter, J., 2005. Flutter-margin method accounting for modal parameter uncertainties. Journal of Aircraft 42, 1236–1243.

Poirel, D., Harris, Y., Benaissa, A., 2008. Self-sustained aeroelastic oscillations of a naca0012 airfoil at low-to-moderate reynolds numbers. Journal of Fluids and Structures 24, 700–719.

Pomeau, Y., Manneville, P., 1980. Intermittent transition to turbulence in dissipative dynamical systems. Communications in Mathematical Physics 74, 189–197.

Price, S., Keleris, J., 1996. Nonlinear dynamics of an airfoil forced to vibrate in dynamic stall. Journal of Sound and Vibration 194 (2), 265–283.

Price, S. J., Lee, B. H. K., 1993. Evaluation and extension of the flutter-margin method for flight flutter prediction. Journal of Aircraft 30, 395–402.

Price, T. J., Mullin, T., 1991. An experimental observation of a new type of intermittency. Physica D 48, 29–52.

Richardson, L. F., 1993. Chaos in Dynamical Systems. Cambridge University Press, Cambridge, UK.

Sarkar, S., Bijl, H., 2008. Nonlinear aeroelastic behavior of an oscillating airfoil during stall induced vibration. Journal of Fluids and Structures 24, 757–777.

Schuster, H., Just, W., 2006. Deterministic chaos: An introduction. John Wiley and Sons.

Strganac, T., Platanitis, G., 2001. Wind tunnel testing of the nasa-dfrc

flutterometer using a two dof wing section. Tech. rep., NASA, USA, http://ntrs.nasa.gov/archive/nasa/casi.ntrs.nasa.gov/20010097722.pdf.

Surovyatkina, E., 2005. Prebifurcation noise amplification and noise-dependent hysteresis as indicators of bifurcations in nonlinear geophysical systems. Nonlinear processes geophysics 12 (1), 25–29.

Takens, F., 1985. Detecting strange attractors in turbulence. In: David, R., Young, L. (Eds.), Dynamical Systems and Turbulence. Vol. 898 of Lecture Notes in Mathematics. Springer, Warwick, pp. 366–381.

Wiesenfeld, K., 1985. Noisy precursors of nonlinear instabilities. Journal of Statistical Physics 38, 1071–1097.

Yoon, Y., Ibrahim, R., 1995. Parametric random excitation of nonlinear coupled oscillators. Nonlinear Dynamics 8, 385–413.

Zhang, P., Huang, S., 2011. Review of aeroelasticity for wind turbine: Current status, research focus and future perspectives. Frontiers in Energy 5 (4), 419–434.

Zimmerman, N., Weissenburger, J., 1964. Prediction of flutter onset speed based on flight testing at subcritical speeds. Journal of Aircraft 1 (4), 190–202.